Available online at www.sciencedirect.com
SCIENCE DIRECT®
Bioorganic & Medicinal Chemistry
ELSEVIER
Bioorganic & Medicinal Chemistry 12 (2004) 1737–1749

Inhibition of the complete set of mammalian secreted phospholipases A_2 by indole analogues: a structure-guided study☆

Brian P. Smart,[a] Ying H. Pan,[b] Amanda K. Weeks,[a] James G. Bollinger,[a] Brian J. Bahnson[b,*] and Michael H. Gelb[a,*]

[a]*Departments of Chemistry and Biochemistry, University of Washington, Seattle, WA 98195, USA*
[b]*Departments of Chemistry and Biochemistry, University of Delaware, Newark, DE 19716, USA*

Received 20 November 2003; accepted 7 January 2004

Abstract—Structure-guided design was employed in a search for potent and selective inhibitors of mammalian secreted phospholipases A_2 (sPLA$_2$s). Using the X-ray structures of human groups IIA and X sPLA$_2$s (hGIIA and hGX) as templates, homology structural models were made for the other human and mouse sPLA$_2$s (hGIB, mGIB, mGIIA, mGIIC, hGIID, mGIID, hGIIE, mGIIE, hGIIF, mGIIF, hGV, mGV, and mGX). Me-Indoxam is a previously discovered indole analogue that binds tightly to many sPLA$_2$s, and the X-ray structure of the hGX-Me-Indoxam complex was determined at a resolution of 2.0 Å. Modeling suggests that the residues near the N_1-substituent of Me-Indoxam vary significantly among the mammalian sPLA$_2$s, and therefore a library of 83 N_1-variants was prepared by parallel synthesis. Several Me-Indoxam analogues bearing a 4-(2-oxy-ethanoic acid) side chain were potent inhibitors (IC_{50} <0.05 μM) of hGIIA, mGIIA, mGIIC, hGIIE, mGIIE, hGV, and mGV, while they displayed intermediate potency (0.05–5 μM) against hGIB, mGIB, hGX, and mGX, and poorly inhibited (>5 μM) hGIID, mGIID, hGIIF, and mGIIF. Me-Indoxam analogues bearing a 5-(4-oxy-butanoic acid) side chain were generally less potent inhibitors. Although no compounds were found to be highly specific for a single human or mouse sPLA$_2$, combinations of Me-Indoxam analogues were discovered that could be used to distinguish the action of various sPLA$_2$s in cellular events. For example, Me-Indoxam and compound **5** are approximately 5-fold more potent on hGIIA than on hGV, and compound **21** is 10-fold more potent on hGV versus hGIIA.

1. Introduction

The phospholipase A_2 class of enzymes catalyze the hydrolysis of the *sn*-2 ester of glycero-phospholipids to release fatty acids and lysophospholipids.[1] One or more of these enzymes is thought to initiate pro-inflammatory cascades by liberating arachidonic acid from membrane phospholipids for the biosynthesis of the eicosanoids (prostaglandins, leukotrienes, and others). The current thinking is that arachidonic acid liberation from the membranes of mammalian cells is catalyzed by the 87-kDa cytosolic phospholipase A_2 (group IVA) and by one or more low molecular weight, secreted phospholipases A_2 (sPLA$_2$s).[2,3] Understanding the role of sPLA$_2$s in this process is complicated by the fact that mammals contain a large number of these enzymes. Humans contain the groups IB, IIA, IID, IIE, IIF, III, V, X, and XIIA sPLA$_2$s (designated hGIB, hGIIA, etc.), whereas the mouse contains all of these sPLA$_2$s (designated mGIB, mGIIA, etc.) plus the group IIC enzyme (which is present in the human genome as a pseudogene).[4,5] Deciphering the role played by sPLA$_2$s in arachidonic acid release as well as in other physiological events would be greatly aided by the availability of potent and specific inhibitors of each mammalian homologue.

Of the numerous known sPLA$_2$ inhibitors, many are non-specific agents that act by perturbing the physical structure of the membrane substrate.[6] sPLA$_2$s are water-soluble enzymes that must bind to the membrane surface to access their water-insoluble substrates, (interfacial enzymes).[7] Methods have been developed for the proper quantitative analysis of inhibitors of

☆Supplementary data associated with this article can be found, in the online version at, doi:10.1016/j.bmc.2004.01.022

*Corresponding author. Tel.: +1-206-543-7142; fax: +1-206-685-8665; e-mail: gelb@chem.washington.edu

0968-0896/$ - see front matter © 2004 Elsevier Ltd. All rights reserved.
doi:10.1016/j.bmc.2004.01.022

interfacial enzymes that allow 'true', active site-directed, competitive inhibitors to be investigated.[6,8,9] Inhibitors that have been convincingly established to be potent and active site-directed competitive inhibitors of $sPLA_2$s either by proper kinetic analysis or by determination of the enzyme-inhibitor X-ray structure include phospholipid analogues (i.e., *sn*-2 amides and phosphonates)[10–14] as well as non-phospholipid analogues including the plant-derived alkaloid aristolochic acid,[15] 1,3-dioxane-4,6-dione-5-carboxamides,[16,17] fatty acid amides,[18] aromatic sulfonamides (i.e., SB-203347),[19] plant-derived sterols,[20] bis-carboxylates,[21,22] complex poly-*p*-hydroxy benzoate natural products,[23–25] highly substituted pyrazoles,[26] short peptides,[27,28] vitamin E analogues,[29] and indole analogues.[30–33] The X-ray structure of some of these compounds bound to hGIIA, porcine and bovine pancreatic $sPLA_2$s, and venom $sPLA_2$s have been determined.[15,17,27–30,34–41]

Of these $sPLA_2$ inhibitors, the indole analogues developed by workers at Lilly and Shionogi laboratories are particularly appealing for further study as they appear to have properties most suitable for use in studies with cultured mammalian cells and are the most generally potent among the full set of human and mouse $sPLA_2$s.[42] We have tested the indole analogue Me-Indoxam (Fig. 1) on all of the human and mouse $sPLA_2$s except the human and mouse group III and mouse group XIIA enzymes, and found it to be a potent inhibitor of mGIIA, hGIIA, mGIIC, mGIIE, hGIIE, mGV, and hGV ($IC_{50} \sim 0.01$–0.02 μM), and a modestly potent inhibitor of mGIB, hGIB, mGX, and hGX ($IC_{50} \sim 0.1$–1 μM).[42] On the other hand Me-Indoxam is a poor inhibitor of mGIID, hGIID, mGIIF, hGIIF, and hGXIIA ($IC_{50} > 10$ μM).[42]

The groups V and X $sPLA_2$s are particularly appealing for further study because these enzymes display high enzymatic activity when added exogenously to a variety of mammalian cells,[43–48] whereas the other mammalian $sPLA_2$s are poorly active in this assay[42] (the human and mouse group III enzymes remain to be analyzed on mammalian cells). These two $sPLA_2$s display the unique ability to bind to phosphatidylcholine-rich vesicles in vitro, which accounts for their ability to act on the phosphatidylcholine-rich outer leaflet of the mammalian cell plasma membrane.[42–45] Thus, among the $sPLA_2$ family members, group V and X enzymes seem to be the strongest candidates for playing a role in arachidonic acid liberation for eicosanoid production. For example, a role for mGV in lipopolysaccharide-induced arachidonic acid release from a murine macrophage-like cell line has been reported.[49] The group V and X $sPLA_2$s also show relatively high activity on serum lipoproteins, and may play a role in the development of atherosclerosis.[50,51]

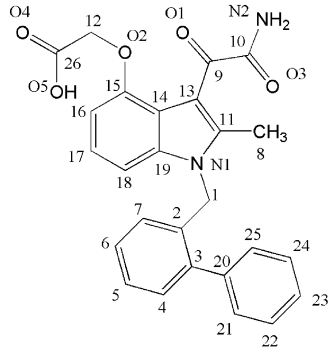

Figure 1. Structure of Me-Indoxam. Atom labels are as given in the pdb file (except for carbons which are labeled C1, C2, etc., whereas they are labeled 1, 2, 3, etc. in the figure). The atom numbering of the indole ring is different than the conventional IUPAC ring numbering. The latter is used to name the compounds synthesized in this study.

In the present study, we extend our structural studies of hGX[52] by reporting the 2.0 Å X-ray crystal structure of this $sPLA_2$ complexed with Me-Indoxam. This structure was then used as a guide for preparing analogues of the lead compound Me-Indoxam with the hope of identifying compounds with improved potency and specificity for one or more of the various human and mouse $sPLA_2$s. We report the preparation, by small-scale, parallel organic synthesis, of a library of 83 Me-Indoxam analogues, and provide inhibition values of many of these compounds toward the full set of human and mouse $sPLA_2$s.

2. Results

2.1. Crystal structure of the complex of hGX with Me-Indoxam

The X-ray crystal structure of hGX-Me-Indoxam was solved in a protein crystal form with two independent subunits in the asymmetric unit. The overall structure is well refined with good geometry with an $R_{working}$ of 0.219 and an R_{free} of 0.267. These statistics are similar to the converged $R_{factors}$ for the ligand free form of hGX that was previously reported from a protein crystal also with symmetry of the $C222_1$ space group and similar unit cell lengths.[52] Furthermore, there are parallels between the two structures with one of the two subunits in each structure exhibiting more disorder than the other, with a notable increase in the individual B-factors. Importantly, the 2-phenyl-benzyl group of the Me-Indoxam inhibitor is well ordered in subunit A and completely disordered in subunit B. The probable cause of this phenomenon is a difference in protein–protein crystal contacts between the two subunits, particularly near the 2-phenyl of the 2-phenyl-benzyl group of the inhibitor. This observed disorder in subunit B indicates the lack of multiple contacts between the protein and the 2-phenyl group of the N_1-substituent of the inhibitor bound to the same subunit. In our design of inhibitors, we hoped to take advantage of the N_1-substituent with a goal to achieve inhibitors that are specific for the various $sPLA_2$ enzymes. For the remainder of the structure description, the more ordered subunit A will be used for analyses and figures.

The Me-Indoxam inhibitor is complexed to the catalytic calcium through interactions between the amide carbonyl oxygen and the carboxyl oxygen atoms. A simu-

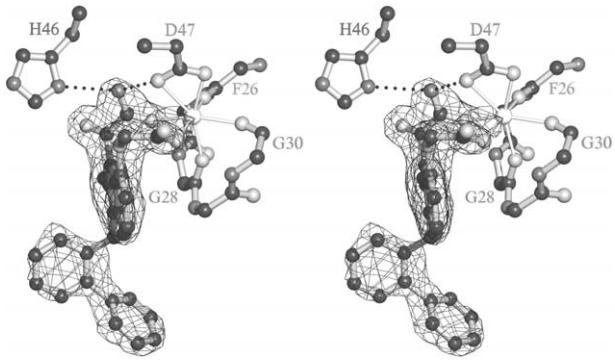

Figure 2. Stereo ball and stick depiction of the hGX-Me-Indoxam complex. The active site is shown including residues H46 and D47, the Ca^{2+}-binding loop and the competitive inhibitor Me-Indoxam. The Ca^{2+} is seven coordinate with three carbonyl backbone ligands (F26, G28, and G30), a bidentate coordination from D47, and coordination to the amide carbonyl oxygen and carboxyl oxygen atoms of Me-Indoxam. Hydrogen bonding of the nitrogen and oxygen atoms of H46 and D47, respectively, are shown by dotted lines. Difference electron density from a composite simulated annealing omit map contoured at 1.0 sigma is displayed around the Me-Indoxam ligand (coefficients 2Fo–Fc). The figure was rendered using the programs MOLSCRIPT,[62] POVSCRIPT (http://people/brandeis.edu/~fenn/povscript/), and POVRAY (http://www.povray.org).

lated annealing omit map of the active site (Fig. 2) demonstrates a well refined structure and provides convincing evidence of the proper modeling of each atom of the Me-Indoxam inhibitor in subunit A of the crystal structure. The resulting calcium coordination of hGX $sPLA_2$ shows the typical 7-coordinate geometry of a ligand bound form of the $sPLA_2$ enzyme[37] as shown in Figure 2. Additional hydrogen bonds exist between the hydrogen on the amide nitrogen of Me-Indoxam and the residues His-46 and Asp-47. The only other hydrogen bonding interactions come from three water molecules that are interacting with the carbonyl oxygen of the carboxyl group of Me-Indoxam. The balance of interactions come from hydrophobic interactions with side chains from residues Ile-2, Leu-5, Ala-6, Met-21, Gly-28, Leu-29, Gly-30, Cys-43, Tyr-50, and Ile-94 as shown in Figure 3. These side chain interactions form the basis of predicted binding affinity differences of Me-Indoxam between the various sequences for the $sPLA_2$ enzymes (discussed below).

The surface of the hGX $sPLA_2$ that binds to lipid water interfaces (i-face) is composed of polar and non-polar residues and displays a preference to zwitterionic interfaces.[52] The 2-phenyl group of the 2-phenyl-benzyl group of the Me-Indoxam inhibitor protrudes out of the enzyme active site opening. The minimal protein side-chain interactions with the 2-phenyl group of Me-Indoxam are consistent with an observation of a disordered N_1-substituent in subunit B of this structure. Furthermore, the hGX-Me-Indoxam inhibitor complex suggests that for the enzyme-inhibitor complex bound to the membrane surface, the 2-phenyl of the 2-phenyl-benzyl group penetrates into the membrane interface, possibly the polar head group region or just below this region.

2.2. Design of the Me-Indoxam library

We desired to prepare Me-Indoxam analogues with improved potency and selectivity for the various mammalian $sPLA_2$s. The X-ray structures of groups I, II, and X $sPLA_2$s show that these enzymes are structurally related,[52,53] and based on sequence homology we anticipate that the structure of group V $sPLA_2$s will also be similar. We built homology structural models of several mammalian $sPLA_2$s (hGIB, mGIB, mGIIA, mGIIC, hGIID, mGIID, hGIIE, mGIIE, hGIIF, mGIIF, hGV, mGV, and mGX) using the X-ray structures of hGIIA and hGX as templates. This was done with the Insight-II software (MSI) simply by replacing peptide segments of hGIIA and hGX with the homologous segments of the other $sPLA_2$s. Many of the active site residues are conserved among all the $sPLA_2$s, and no attempt was made to minimize the energy of the structural models using molecular dynamics. Addition-

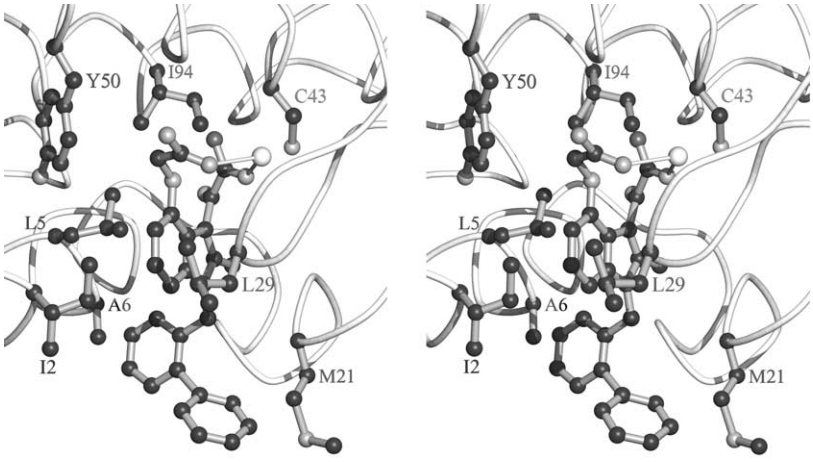

Figure 3. hGX-Me-Indoxam contacts. Side chain residues of hGX that lie within 4 Å of Me-Indoxam are displayed in ball and stick format for residues Ile-2, Leu-5, Ala-6, Met-21, Leu-29, Cys-43, Tyr-50, and Ile-94. Coordination of Me-Indoxam to the Ca^{2+} is shown. The side chain contacts from His-46 and Asp-47 and main chain contacts within residues of the calcium binding loop (residues 26–30) are not shown for clarity and can be observed in Figure 2. Cys-43 is disulfide linked to another cysteine residue (not shown).

ally, no attempt to model the structure of hGIII and hGXIIA was made since these enzymes show amino acid sequence homology to the groups I, II, V and X $sPLA_2$s only in short stretches that include the catalytic residues. With notable exceptions (see below), the residues that contact the indole core, the glyoxamide side chain, and the 4-(2-oxy-ethanoic acid) side chain of Me-Indoxam are well conserved among the groups I, II, V, and X $sPLA_2$s. On the other hand, residues that are likely to contact the 2-phenyl-benzyl side chain attached to the N_1-position of Me-Indoxam differ significantly among the various group I, II, V, and X $sPLA_2$s. Thus, it seemed reasonable to prepare a library of Me-Indoxam analogues in which the N_1-substituent is varied. Since the analogue of Me-Indoxam in which the 4-(2-oxy-ethanoic acid) side chain is replaced with hydrogen and the longer 4-oxy-butanoic acid side chain is present at the 5-position of the indole core is also reported to be a potent inhibitor of hGIIA,[54] we also prepared a library of these compounds in which the N_1-substituent was varied.

2.3. Chemistry

Figure 4 shows the synthetic scheme used to prepare a library of indole analogues containing the common functionalities, a 2-methyl group, a 3-glyoxamide side chain and either a 4-(2-oxy-ethanoic acid) or a 5-(4-oxy-butanoic acid) side chain, and with varying substituents at the N_1-position. The N_1-substituent is introduced late in the synthesis, which facilitated the preparation of a large number of analogues in which this substituent was varied. Commercially available 4- and 5-hydroxy-2-methyl indoles **(A)** and **(E)**, respectively (Fig. 4), were treated with potassium carbonate in refluxing acetone, resulting in selective deprotonation of the hydroxyl group. Alkylation of the alkoxide with *tert*-butyl 2-bromoacetate or *tert*-butyl 4-bromobutanoate provided indoles **(B)** and **(F)**, respectively. The 3-glyoxamide side chain was added to the indole in two steps. First, indole **(B)** or **(F)** was added to a dilute solution of oxalyl chloride in CH_2Cl_2. High dilution conditions were necessary to avoid the troublesome dimerization of the indole.

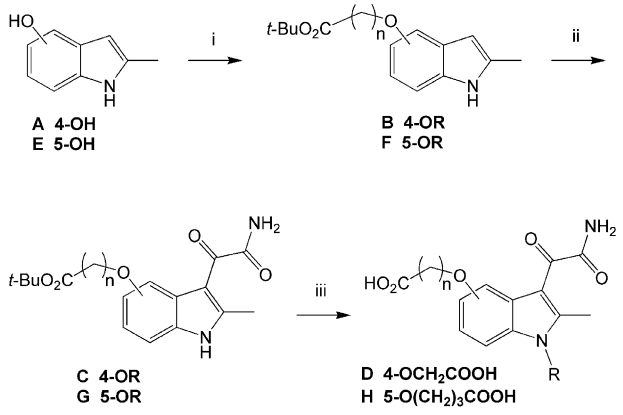

Figure 4. Synthesis of Me-Indoxam analogues. The reagents used are: (i) K_2CO_3, $Br(CH_2)_nCO_2t$-Bu ($n=1$ or 3), acetone, reflux; (ii) oxalyl chloride, CH_2Cl_2 followed by NH_3; (iii) NaH, RBr, THF followed by neat CF_3CO_2H.

Next, the acyl chloride intermediate was converted to the amide by bubbling ammonia gas into the solution. Common intermediates **(C)** and **(G)** were used to prepare the library of Me-Indoxam analogues **(D)** and **(H)**, respectively. A single solution of **(C)** or **(G)** in THF was treated with NaH leading to deprotonation of the N_1-hydrogen. This mixture was distributed into several small vials and allowed to react with various alkyl bromides to form the N_1-substituted indole analogues. Treatment with neat trifluoroacetic acid led to deprotection of the *tert*-butyl ester of the side chain at the 4- or 5-position of the indole ring to give the desired library members **(D)** and **(H)**. Each compound was purified by HPLC and confirmed to have the correct structure by electrospray ionization mass spectrometry. The structure of the 48 indole analogues with a 4-(2-oxy-ethanoic acid) chain (compounds **1**–**48**) are shown in Table 1, and the structures of the 35 indole analogues with a 5-(4-oxy-butanoic acid) chain (compounds **49**–**83**) are shown in Table 3.

We desired an accurate and rapid method to quantify the amount of Me-Indoxam analogues that were prepared by multiple, small-scale, parallel organic synthesis. Thus, we used low specific activity, carbon-14-labeled oxalyl chloride to form the glyoxamide side chain, which permitted the concentration of Me-Indoxam analogues in stock solutions to be quantified by scintillation counting. Labeled oxalyl chloride was synthesized from commercially available [^{14}C]oxalic acid by reaction with phosphorous pentachloride.

2.4. $sPLA_2$ inhibition studies

We developed a high throughput, fluorometric assay of $sPLA_2$s that can be carried out in multi-well plates.[43] The full set of 48 Me-Indoxam analogues with a 4-(2-oxy-ethanoic acid) side chain were tested on the set of human $sPLA_2$s (hGIB, hGIIA, hGIID, hGIIE, hGIIF, hGV, hGX, and hGXIIA) (Table 1) and on the set of mouse $sPLA_2$s (mGIB, mGIIA, mGIIC, mGIID, mGIIE, mGIIF, mGV, and mGX) (Table 2). Indole analogues were tested at a single concentration and re-tested at a second concentration if inhibition approached 100% or if inhibition was $<30\%$. Studies with mGXIIA were not carried out because the Me-Indoxam analogues were uniformly poor inhibitors of hGXIIA, and mGXIIA is 96% identical in amino acid sequence to hGXIIA (the active site residues of these two enzymes are identical). Studies with hGIII were limited to testing only analogue **21** because of limited amount of enzyme. It is anticipated that other indole analogues would not be potent against hGIII given that indole **21** is a weak inhibitor, and that the active site structure of hGIII is predicted to be different from that of groups I, II, V, and X $sPLA_2$s (based on the X-ray structure of the related group III $sPLA_2$ from honey bee venom[36]).

Me-Indoxam analogues with a 5-(4-oxy-butanoic acid) side chain were tested (Table 3) and were found to be much less potent $sPLA_2$ inhibitors than the 4-(2-oxy-ethanoic acid)-containing analogues. Thus the former were tested only on hGIIA and hGX $sPLA_2$s.

Table 1. Inhibition of human sPLA$_2$s by indoles bearing a 4-(2-oxy-ethanoic acid) side chain

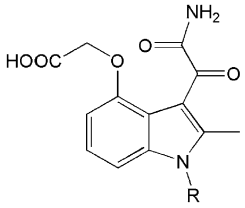

R Group	Compd	% Inhibition against human sPLA$_2$											
		IB 0.5 μM	IIA 0.33 μM	IIA 0.025 μM	IID 5 μM	IIE 0.5 μM	IIE 0.025 μM	IIF 5 μM	III 5 μM	V 0.33 μM	V 0.10 μM	X 0.33 μM	XIIA 5 μM
2,6-Cl_2-$C_6H_3CH_2$	1	71	100	45	17	98	68	46		95	86	30	6
Phthalimido$(CH_2)_4$	2	25	2	5	9	86	17	37		50	34	15	7
$C_6F_5CH_2$	3	63	33	6	20	72	0	14		32	3	9	9
4-Br-$C_6H_4CH_2$	4	78	100	53	63	96	80	65		93	85	29	31
$C_6H_5COCH_2$	5	14	61	27	0	36	0	22		10	8	0	14
3-(CH_2Br)-$C_6H_4CH_2$	6	37	86	29	9	96	81	44		82	59	19	2
3-Cl-$C_6H_4CH_2$	7	59	96	30	31	100	86	38		93	81	33	16
2-NapthaleneCH_2	8	58	97	33	49	100	80	60		93	84	15	24
4-CN-$C_6H_4CH_2$	9	36	29	4	34	100	42	52		69	44	13	13
2-CN-$C_6H_4CH_2$	10	10	82	23	0	100	84	23		47	20	0	27
3-CN-$C_6H_4CH_2$	11	9	86	29	0	95	47	22		71	37	1	11
$(CH_3)_2CHCH_2$	12	28	64	31	20	81	13	30		63	33	26	24
2-(OCH_3)-5-(NO_2)-$C_6H_3CH_2$	13	37	7	0	16	49	0	16		4	0	2	0
3-Br-$C_6H_4CH_2$	14	59	95	27	70	100	88	44		93	84	37	13
2-Br-$C_6H_4CH_2$	15	50	100	22	26	100	96	45		78	49	26	18
2-F-$C_6H_4CH_2$	16	70	100	37	41	100	96	40		90	75	40	9
4-F-$C_6H_4CH_2$	17	67	80	34	52	97	69	41		88	73	24	9
3-(NO_2)-$C_6H_4CH_2$	18	24	57	32	5	97	46	29		82	46	30	1
4-(7-CH_3O)-coumarinylCH_2	19	18	9	0	44	6	2	12		2	20	0	2
1-(8-CH_2Br)-naphthaleneCH_2	20	24	24	2	37	91	18	52		23	5	18	8
(*S*)-(+)-$CH_3CH_2CH(CH_3)CH_2$	21	55	22	0	0	94	0	37	8	86	57	33	19
2-Cl-$C_6H_4CH_2$	22	30	91	31	52	100	99	43		88	57	36	12
PhthalimidoCH_2	23	9	0	9	38	53	0	17		6	2	0	3
2-(CF_3)-$C_6H_4CH_2$	24	29	93	30	23	100	93	31		79	48	19	14
2,4-F_2-$C_6H_3CH_2$	25	78	84	7	89	98	82	41		93	70	27	13
2,5-F_2-$C_6H_3CH_2$	26	62	76	1	34	98	52	22		80	44	13	10
2,6-F_2-$C_6H_3CH_2$	27	79	91	12	34	98	82	44		92	68	16	11
3,4-F_2-$C_6H_3CH_2$	28	32	84	22	48	96	54	31		94	60	12	7
2,3-F_2-$C_6H_3CH_2$	29	73	96	15	29	99	85	37		98	68	47	16
3,5-F_2-$C_6H_3CH_2$	30	55	84	20	60	90	16	22		55	4	24	6
3-(CF_3)-$C_6H_4CH_2$	31	55	97	30	0	95	81	8		92	76	18	10
4-(CF_3)-$C_6H_4CH_2$	32	60	83	15	23	100	62	41		79	49	3	19
2-((2-CH_2Br)-C_6H_4)-$C_6H_4CH_2$	33	83	97	25	43	87	23	51		95	66	17	33
3-(OCF_3)-$C_6H_4CH_2$	34	49	97	53	55	94	89	49		94	75	32	17
3-I-$C_6H_4CH_2$	35	59	98	51	59	96	89	58		92	75	20	19
2-(CF_3)-4-F-$C_6H_4CH_2$	36	36	93	45	7	95	77	26		64	43	0	13
2,3,6-F_3-$C_6H_2CH_2$	37	56	84	9	8	94	63	19		76	20	4	15
2,5-(CF_3)$_2$-$C_6H_3CH_2$	38	15	7	1	45	54	0	23		2	0	0	14
4-(CH_3)-$C_6H_4CH_2$	39	46	88	9	30	100	85	38		85	62	5	14
CH_3CH_2	40	0	39	13	27	17	0	3		1	1	0	10
$CH_3(CH_2)_2$	41	15	51	10	45	66	0	5		37	2	0	5
$CH_3(CH_2)_3$	42	72	69	18	33	84	0	26		52	31	4	0
$CH_3(CH_2)_4$	43	63	57	4	77	71	0	26		26	21	15	5
$CH_3(CH_2)_5$	44	66	79	9	78	84	3	43		23	35	15	8
$CH_3(CH_2)_6$	45	75	89	22	62	90	21	50		60	49	35	8
$CH_3(CH_2)_7$	46	80	100	59	100	92	31	60		64	53	42	15
$C_6H_5CH_2$	47	68	82	24	29	97	84	42		73	65	22	0
	48												
2-(C_6H_5)-$C_6H_4CH_2$	Me-Indoxam	84	100	58	9	100	91	34		91	75	57	25

Analyses were performed in at least duplicate for hGIIA, hGV, and hGX sPLA$_2$ enzymes.

Table 2. Inhibition of mouse sPLA$_2$s by indoles bearing a 4-(2-oxy-ethanoic acid) side chain

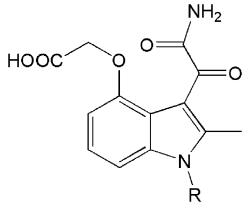

R Group	Compd	% Inhibition against mouse sPLA$_2$							
		IB 0.5 μM	IIA 0.025 μM	IIC 0.025 μM	IID 5 μM	IIE 0.025 μM	IIF 5 μM	V 0.333 μM	X 1.0 μM
2,6-Cl_2-$C_6H_3CH_2$	1	96	85	70	27	56	2	95	70
Phthalimido$(CH_2)_4$	2	66	17	42	17	21	4	55	35
$C_6F_5CH_2$	3	69	8	55	14	29	8	31	38
4-Br-$C_6H_4CH_2$	4	89	88	78	85	61	30	97	61
$C_6H_5COCH_2$	5	17	0	15	15	19	6	7	7
3-(CH_2Br)-$C_6H_4CH_2$	6	52	47	64	16	62	5	87	51
3-Cl-$C_6H_4CH_2$	7	84	75	83	59	31	5	92	68
2-NapthaleneCH_2	8	86	83	82	92	27	30	87	64
4-CN-$C_6H_4CH_2$	9	54	29	42	25	6	0	75	49
2-CN-$C_6H_4CH_2$	10	31	34	52	11	45	0	66	42
3-CN-$C_6H_4CH_2$	11	27	17	11	12	12	4	63	33
$(CH_3)_2CHCH_2$	12	59	10	38	64	0	15	73	34
2-(OCH_3)-5-(NO_2)-$C_6H_3CH_2$	13	57	4	14	12	4	8	5	4
3-Br-$C_6H_4CH_2$	14	78	75	86	56	26	7	96	73
2-Br-$C_6H_4CH_2$	15	81	74	93	33	45	12	86	73
2-F-$C_6H_4CH_2$	16	81	78	99	50	51	8	94	77
4-F-$C_6H_4CH_2$	17	76	78	82	39	32	3	88	47
3-(NO_2)-$C_6H_4CH_2$	18	31	36	33	21	20	1	74	35
4-(7-CH_3O)-coumarinylCH_2	19	20	0	12	18	0	13	8	7
1-(8-CH_2Br)-naphthaleneCH_2	20	73	8	27	12	0	3	29	21
(*S*)-(+)-$CH_3CH_2CH(CH_3)CH_2$	21	60	16	59	58	16	5	87	55
2-Cl-$C_6H_4CH_2$	22	81	75	95	44	62	8	91	69
PhthalimidoCH_2	23	9	11	18	19	10	2	4	13
2-(CF_3)-$C_6H_4CH_2$	24	62	46	78	3	60	4	84	69
2,4-F_2-$C_6H_3CH_2$	25	78	66	86	40	56	8	95	54
2,5-F_2-$C_6H_3CH_2$	26	74	49	88	32	34	0	77	58
2,6-F_2-$C_6H_3CH_2$	27	77	72	83	30	45	0	89	80
3,4-F_2-$C_6H_3CH_2$	28	73	45	61	25	26	0	76	41
2,3-F_2-$C_6H_3CH_2$	29	72	73	92	29	57	8	93	70
3,5-F_2-$C_6H_3CH_2$	30	63	33	67	30	13	4	56	47
3-(CF_3)-$C_6H_4CH_2$	31	63	54	67	49	47	10	92	63
4-(CF_3)-$C_6H_4CH_2$	32	74	56	48	45	35	5	73	33
2-((2-CH_2Br)-C_6H_4)-$C_6H_4CH_2$	33	84	43	89	11	31	40	90	71
3-(OCF_3)-$C_6H_4CH_2$	34	68	66	73	62	37	16	87	51
3-I-$C_6H_4CH_2$	35	71	67	83	56	35	32	91	64
2-(CF_3)-4-F-$C_6H_4CH_2$	36	71	47	68	17	37	13	66	23
2,3,6-F_3-$C_6H_2CH_2$	37	68	57	73	16	27	5	71	62
2,5-(CF_3)$_2$-$C_6H_3CH_2$	38	37	0	16	13	7	24	14	10
4-(CH_3)-$C_6H_4CH_2$	39	67	74	83	46	43	9	85	59
CH_3CH_2	40	18	0	6	48	4	11	12	2
$CH_3(CH_2)_2$	41	58	5	31	74	8	10	44	8
$CH_3(CH_2)_3$	42	79	35	55	71	10	4	70	40
$CH_3(CH_2)_4$	43	79	37	56	40	0	11	58	30
$CH_3(CH_2)_5$	44	80	59	69	71	0	13	65	39
$CH_3(CH_2)_6$	45	87	71	80	89	17	23	74	40
$CH_3(CH_2)_7$	46	86	82	86	95	6	36	82	54
$C_6H_5CH_2$	47	72	72	85	34	69	11	85	69
	48								
2-(C_6H_5)-$C_6H_4CH_2$	Me-Indoxam	90	81	92	39	28	34	94	67

Table 3. Inhibition of $sPLA_2$s by indoles bearing a 5-(4-oxy-butanoic acid) side chain

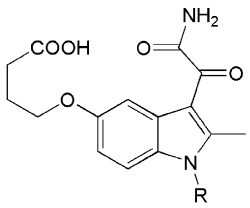

R Group	Compd	% Inhibition	
		hGIIA 1 μM	hGX 1 μM
2,6-Cl_2-$C_6H_3CH_2$	49	85	11
$C_6F_5CH_2$	50	26	4
4-Br-$C_6H_4CH_2$	51	83	20
$C_6H_5COCH_2$	52	37	43
3-Cl-$C_6H_4CH_2$	53	87	36
2-NapthaleneCH_2	54	93	4
4-CN-$C_6H_4CH_2$	55	33	20
2-CN-$C_6H_4CH_2$	56	0	13
3-CN-$C_6H_4CH_2$	57	10	10
$(CH_3)_2CHCH_2$	58	29	0
2-(OCH_3)-5-(NO_2)-$C_6H_3CH_2$	59	63	20
3-Br-$C_6H_4CH_2$	60	83	11
2-Br-$C_6H_4CH_2$	61	75	43
4-F-$C_6H_4CH_2$	62	49	26
3-(NO_2)-$C_6H_4CH_2$	63	5	10
4-(7-CH_3O)-coumarinylCH_2	64	0	18
2-Cl-$C_6H_4CH_2$	65	77	0
PhthalimidoCH_2	66	0	18
2-(CF_3)-$C_6H_4CH_2$	67	8	6
2,4-F_2-$C_6H_3CH_2$	68	90	78
2,5-F_2-$C_6H_3CH_2$	69	27	30
2,6-F_2-$C_6H_3CH_2$	70	13	26
3,4-F_2-$C_6H_3CH_2$	71	16	44
2,3-F_2-$C_6H_3CH_2$	72	55	13
3,5-F_2-$C_6H_3CH_2$	73	79	68
3-(CF_3)-$C_6H_4CH_2$	74	46	59
4-(CF_3)-$C_6H_4CH_2$	75	23	30
2-((2-CH_2Br)-C_6H_4)-$C_6H_4CH_2$	76	0	32
3-(OCF_3)-$C_6H_4CH_2$	77	77	32
2-(CF_3)-4-F-$C_6H_4CH_2$	78	3	15
4-(CH_3)-$C_6H_4CH_2$	79	89	27
$CH_3(CH_2)_3$	80	29	28
$CH_3(CH_2)_4$	81	7	25
$CH_3(CH_2)_5$	82	8	19
$CH_3(CH_2)_6$	83	31	36

Analyses were performed in at least duplicate for hGIIA and hGX $sPLA_2$ enzymes.

3. Discussion

3.1. Inhibition patterns among $sPLA_2$ enzyme species

The large amount of inhibition data obtained with the 4-(2-oxy-ethanoic acid) analogues and the human $sPLA_2$s (potency of 48 compounds on eight group I, II, V, and X enzymes) is conveniently summarized by the gray scale array shown in Figure 5A. Figure 5B shows the array for the same compounds as inhibitors of the eight mouse $sPLA_2$s. Figure 5C shows a comparison of the results obtained with human and mouse $sPLA_2$s (mGIIC is removed since there is no hGIIC and mGXIIA is removed since inhibition data is not available, see above). The general pattern for potency of inhibition among the various enzyme species is readily apparent from inspection of these arrays and is summarized as follows. For the human $sPLA_2$s, several members of the 48-compound, Me-Indoxam analogue library are potent inhibitors (IC_{50} < 0.05 μM) of hGIIA, hGIIE and hGV. These compounds show intermediate potency against hGIB (several compounds with an IC_{50} = 0.05–0.5 μM) and hGX (several compounds with an IC_{50} = 0.5–5 μM), and are poor inhibitors of hGIID, hGIIF, and hGXIIA (IC_{50} > 5 μM). The same set of Me-Indoxam analogues are potent inhibitors of mGIIA, mGIIC, mGIIE, and mGV (several compounds with an IC_{50} < 0.05 μM), they show intermediate potency toward mGIB (several compounds with an IC_{50} = 0.05–0.5 μM) and mGX (several compounds with an IC_{50} = 0.5–5 μM), and are poor inhibitors of mGIID and mGIIF (IC_{50} > 5 μM). It can be seen from Figure 5C that for each human/mouse orthologue pair, the inhibition potencies for the Me-Indoxam analogues acting on the human $sPLA_2$ matches closely to that measured for its mouse orthologue (hGIB versus mGIB, hGIIA versus mGIIA, hGIID versus mGIID, hGIIE versus mGIIE, hGIIF versus mGIIF, hGV versus mGV, and hGX versus mGX). This is expected given that for each orthologue pair, the active site residues are highly conserved (based on the hGIIA and hGX X-ray structures and the active site models for the remaining groups I, II, V, and X enzymes).

3.2. Interactions between enzyme residues and the indole core of Me-Indoxam and its analogues

The trends in inhibition potency among the different $sPLA_2$ species noted above tend to hold as the N_1-substituent is varied. In addition, the contacts between the glyoxamide and carboxymethyl side chains of Me-Indoxam and the enzyme are conserved among all of the $sPLA_2$s. This suggests that it is the residues that interact with the remaining portion of Me-Indoxam, the indole core, that are responsible for the differences in inhibition potency among the $sPLA_2$ enzyme species. For the hGX-Me-Indoxam complex, these residues are Ile-2, Leu-5, Gly-28, and Leu-29 (Fig. 3). The residues at these positions for all of the human and mouse groups I, II, V, and X $sPLA_2$s are listed in Table 4 (supplemental information). For all of the enzymes, glycine is conserved at position-28. This leaves residues 2, 5, and 29 for further consideration. When residue 5 is a Phe, the edge of this aromatic group would form a favorable interaction with the aromatic face of the indole ring of Me-Indoxam. Such an interaction between two aromatic rings that are perpendicular to each other is thought to be highly favorable.[55] This could explain why Me-Indoxam and many of its analogues are generally potent inhibitors of hGIB, mGIB, hGIIA, mGIIA, mGIIC, hGIIE, and mGIIE, all of which have a Phe-5 (Table 4, supplemental information). Within this group of enzymes, less potent inhibition is seen with hGIB and mGIB. This may be due to the fact that the group IB enzymes have a Val at position-2, which is not quite long enough to contact the indole core of the inhibitor. In contrast, the group IIA, IIC, and IIE $sPLA_2$s contain longer aliphatic side chains

at position-2 (Leu, Ile, and Phe) which are predicted to make a direct contact with the indole core of Me-Indoxam, based on the contact between Ile-2 and inhibitor observed in the hGX-Me-Indoxam X-ray structure. Thus, the combination of Phe-5 and Leu, Ile, or Phe at position-2 seems to provide the most favorable interaction with the indole core of Me-Indoxam. The enzymes hGIID, mGIID, hGIIF, mGIIF, hGX, and mGX all have Leu at position-5 instead of Phe, and this may be the reason that Me-Indoxam and its analogues are generally poor inhibitors of these enzymes. The group V sPLA$_2$s represent an exception to these trends. They have Leu-2, which favors Me-Indoxam binding, but they contain Leu-5 instead of Phe-5, which should disfavor binding and yet many of the Me-Indoxam analogues are potent hGV and mGV inhibitors.

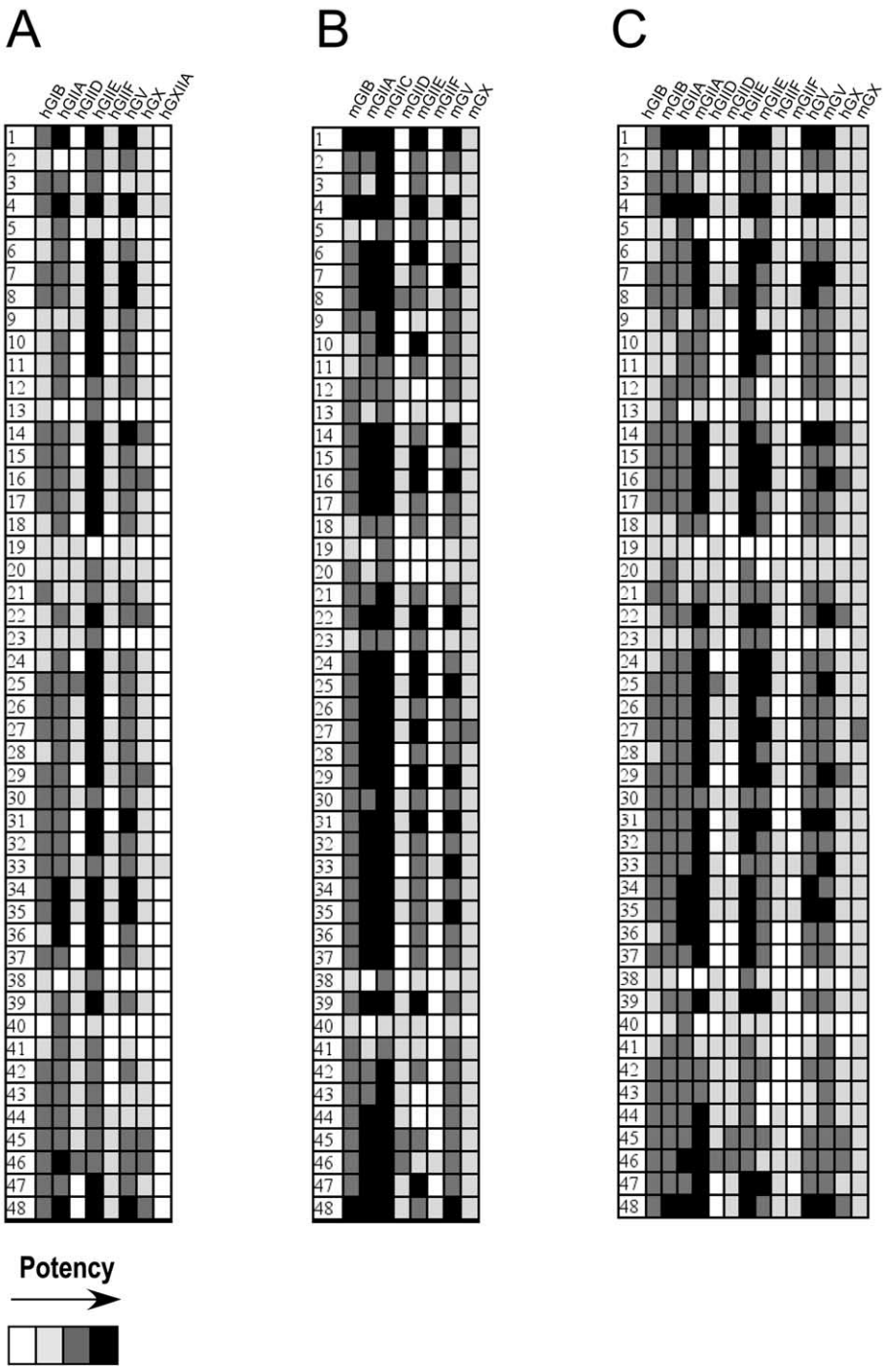

Figure 5. Array of potencies of inhibition of human and mouse sPLA$_2$s by Me-Indoxam and its analogues. Panel A is for the human enzymes indicated along the horizontal top edge of the array, panel B is for the mouse enzymes, and panel C is human and mouse enzymes combined. The vertical edge of the array gives the compound numbers for the Me-Indoxam analogues with the 4-(2-oxy-ethanoic acid) side chain (see Table 1). Inhibition potency was classified into 4 gray scale categories as follows: black is $IC_{50} < 0.05$ μM, dark gray is $IC_{50} = 0.05$–0.5 μM, light gray is $IC_{50} = 0.5$–5 μM, and white is $IC_{50} > 5$ μM.

However, the group V $sPLA_2$s are unique in containing a Trp at position-29, whereas all of the other $sPLA_2$s contain an aliphatic residue at this position (Ile, Leu, Val). The homology models of the group V $sPLA_2$ active sites suggest that the edge of the indole ring of Trp-29 could form a favorable interaction with the face of the indole ring of Me-Indoxam.

3.3. Interaction between enzyme residues and the N_1-substituent of Me-Indoxam and its analogues

The X-ray structure of Me-Indoxam bound to hGX shows that the 2-phenyl group on the N_1-benzyl chain does not form significant interactions with the enzyme (discussed above). This is predicted to be the case for all group I, II, V, and X $sPLA_2$s, based on modeling. This presumably explains why the potency of Me-Indoxam and **47**, which lacks the 2-phenyl group, are similar for all $sPLA_2$s (maximum difference in potency of $\sim$3-fold).

Inspection of the hGX-Me-Indoxam X-ray structure suggests that a 2-, 3- or 4-substituent on the N_1-benzyl group would not influence $sPLA_2$ inhibition potency since these substituents protrude away from the enzyme surface. Indeed compounds **4**, **6**, **7**, **9**–**11**, **14**–**18**, **22**, **24**, **31**–**35**, **39**, and **48,** which contain a single substitution at either the 2-, 3- or 4-position of the N_1-benzyl chain, display similar inhibition potency as compound **47**, which contains an unsubstituted N_1-benzyl chain. This trend is true for all $sPLA_2$s as predicted from the active site modeling. The same applies for disubstituted N_1-benzyl chains that include 2-, 3-, and 4-substituents (compounds **25**, **28**, **29**, and **36**). It is clear from the X-ray structure of the hGX-Me-Indoxam complex as well as the models for the other $sPLA_2$ active sites that compounds **13** and **38** are expected to be generally poor inhibitors, and this was found to be the case. These compounds have an N_1-benzyl group with a 2,5-disubstitution pattern. This leads to a steric clash with the enzyme. If the 2-substituent points away from the enzyme surface, the 5-substituent would clash with Ala-6 of hGX (as well as corresponding residues of the other $sPLA_2$s). Flipping the aromatic ring would relieve the steric clash with the 5-substituent and Ala-6, but would position the 2-substituent in steric clash with the indole ring of Me-Indoxam. Poor inhibition was not observed for compound **26,** which contains the smaller fluorine atoms at the 2- and 5-position. Compounds **1** and **27**, which contain a 2,6-dichloro and 2,6-difluoro pattern of substitution on the benzyl group display similar potency as compound **47**, which contains the unsubstituted benzyl chain. Presumably the fluorine and chlorine substituents cause less steric clash because they are smaller than those present on the poorly active compounds with 2,5-disubstituted benzyl chains (**13** and **38** which contain larger substituents OMe, NO_2, and CF_3).

Indole analogues containing non-benzyl substituents at the N_1-position (**2**, **5**, **8**, **12**, **19**, **20**, **21**, **23**, **40**, **41**, **42**, **43**, **44**, **45**, and **46**) generally display poor inhibition potency against human and mouse $sPLA_2$s. The hGX-Me-Indoxam X-ray structure shows the benzyl group of Me-Indoxam pointing into the hydrophobic cavity of the enzyme and interacting favorably with Ile-2 and Ala-6. However, the non-benzyl substituents either sterically clash with Ala-6 (**8** and **19**) or lose their favorable interaction with Ile-2 and Ala-6 (**2**, **5**, and **12**) of hGX as seen from modeling of these substituents with the hGX-Me-Indoxam X-ray structure and models of the human and mouse groups I, II, V, and X $sPLA_2$s. Indole analogue **23** does not contact Ala-6, but instead its phthalimido group sterically clashes with Leu-29 and Gly-30 of hGX because the methylene group between the N_1-position and the phthalimido group is too short to allow the phthalimido group to protrude out of the active site. Analogue **21** is similar to analogue **12** (branched alkyl group at the N_1-position) except that the side chain is lengthened by one carbon. This re-establishes the favorable interaction with Ala-6 of hGX, as the geometry of the chain rotates to mimic the benzyl substituent of Me-Indoxam. Indole analogues **40**–**46** display increasing inhibition potency against human and mouse group $sPLA_2$s. This is due to the filling of the hydrophobic cavity by the increasing size of the saturated alkyl chains. The favorable interactions with Ile-2 and Ala-6 of hGX (and the corresponding residues of the other $sPLA_2$s modeled) are realized as the chain length is increased to eight carbons. Presumably, after eight carbons this trend would no longer hold, as the remaining methylene groups would protrude out of the cavity and not interact with any protein residues.

3.4. Discovery of compounds useful for cellular studies of $sPLA_2$ function

With the series of Me-Indoxam analogues prepared in the current study, we have not been able to generate compounds that are highly specific for a single human or mouse $sPLA_2$. However, some compounds that will be useful in cell culture studies have been found. For example, the original lead compound Me-Indoxam and compound **5** are $\sim$5-fold more potent on hGIIA than on hGV, and compound **21** was discovered to have a reverse preference (10-fold more potent on hGV compared to hGIIA). Compound **21** was re-tested on all of the human $sPLA_2$s to determine the precise IC_{50} values (based on enzyme activity measured in the presence of five inhibitor concentrations): hGIB, $IC_{50} = 0.77$ μM; hGIIA, $IC_{50} = 1.0$ μM; hGIID, no inhibition at 5 μM; hGIIE, $IC_{50} = 0.04$ μM; hGIIF, no inhibition at 5 μM; hGV, $IC_{50} = 0.1$ μM; hGX, $IC_{50} = 5$ μM; hGXIIA, $<20\%$ inhibition at 5 μM. Thus, Me-Indoxam or compound **5**, when used in combination with compound **21**, should be useful for distinguishing cellular events caused by hGIIA versus hGV.

4. Conclusion

In an attempt to find potent and selective inhibitors of mammalian secretory phospholipases A_2, a library of 83 indole analogues was synthesized and tested against the full set of mouse and human $sPLA_2$s. Homology models of the human and mouse $sPLA_2$s were made based on the X-ray structures of the hGIIA and hGX and

inhibitors were designed with structure-guided techniques. The X-ray structure was determined of Me-Indoxam, an indole analogue that is a competitive tight binding inhibitor of several $sPLA_2$s, and modeling of this structure with the $sPLA_2$ homology models suggests a good deal of variation in the residues surrounding the N_1-position of the indole. Based on this structure and a series of previously published indoles bound to the hGIIA $sPLA_2$, a library was generated by varying the N_1-substituent of the indole and the position and length of the calcium coordinating carboxylate arm. All compounds generated were tested in a fluorometric assay employing vesicles with a pyrenedecanoic acid at the *sn*-2 position of the phospholipid. The structure–activity relationship suggests that a 4-(2-oxy-ethanoic acid) moiety and an N_1-position carrying a substituted benzyl group are the most highly potent against the $sPLA_2$ enzymes. However, 2,5- and 3,6-disubstituted benzyl groups at the N_1-position cause steric clash and significantly diminish the inhibition potency. Although no single compound was highly selective for a single $sPLA_2$ enzyme, a combination of compounds with a 5 to 10-fold inverse selectivity preference for the hGV versus hGIIA was found and should prove useful in cell culture studies.

5. Experimental

5.1. Crystallization and X-ray data collection

The purified recombinant hGX $sPLA_2$ was prepared as described elsewhere.[52] The hGX-Me-Indoxam complex was co-crystallized at ambient temperature in 2 μL hanging drops of a mixture of 1 μL of a pre-equilibrated solution containing 15 mg/mL protein, 0.56 mM Me-Indoxam, 10 mM $CaCl_2$, 10% (v/v) MPD, 0.25% (v/v) DMSO, and 1 μL of a crystallization reservoir solution of 10 mM $CaCl_2$, 12% (w/v) PEG 3500, 10% (v/v) MPD, 2% (v/v) ethylene glycol and 0.2 M Hepes buffer, pH 7.4. Crystals of rectangular shape appeared within a week and were allowed to grow for two weeks before data collection.

X-ray diffraction data were collected on a Rigaku RU-H3R rotating anode generator with a RAXIS IV image plate area detector. Crystals were pre-treated with a cryo-protecting and stabilizing solution made of the crystallization condition reported above with the addition of 10% (v/v) glycerol and flash frozen in the −180 °C nitrogen cryo-stream. X-ray diffraction data were collected from a single crystal that diffracted to a resolution of 1.97 Å. The programs DENZO and SCALEPAK were used for data processing.[56] The data collection statistics are shown in Table 5 (supplemental information). The protein crystal belongs to space group $C222_1$ with 2 copies of the hGX-Me-Indoxam complex in the asymmetric unit.

5.2. X-ray structure solution and refinement

The structure was solved by molecular replacement using the program AMORE[57] using a ligand free structure of hGX[52] (pdb code 1LE6) as the search model. Standard refinement techniques in the program CNS-1.1[58] such as rigid body, positional and simulated annealing refinement were employed during cycles of refinement. Manual model improvement was done using the graphic programs CHAIN[59] and O.[60] The Me-Indoxam ligand was built into one of the two subunits of the protein when the R_{free} and $R_{working}$ were at 0.339 and 0.279, respectively at resolution 2.2 Å. Following a round of refinement, the electron density difference maps (2Fo-Fc) showed clear electron density for the active site ligand. Next, one round of positional and simulated annealing refinement was performed using X-ray diffraction data that was extended to a resolution of 2.0 Å. Electron density difference maps directed the building of a second Me-Indoxam molecule into the second subunit's active site and was refined. Finally, a total of 164 solvent molecules were built into difference electron density (Fo–Fc), and iterative rounds of model adjustment and refinement converged. The final model has a value of R_{free} and $R_{working}$ of 0.269 and 0.221, respectively with good geometry.

5.3. Synthesis of Me-Indoxam analogues

5.3.1. General methods. Unless otherwise noted, all reagents were obtained from commercial suppliers and used without further purification and all non-aqueous reactions were carried out under an argon atmosphere with oven-dried glassware. THF was distilled under argon from sodium/benzophenone and CH_2Cl_2 was distilled over CaH_2 immediately prior to use. Reaction progress was monitored by thin-layer chromatography on Merck $60F_{254}$ silica plates. Unless otherwise specified, extracts were dried over $MgSO_4$ and solvents were removed with a rotary evaporator at aspirator pressure. All compounds were purified by column chromatography using Merck 60 230–400 mesh silica gel. NMR spectra were recorded on Bruker AC-200 (200 MHz) or AC-300 (300 MHz) spectrometers. Unless otherwise specified, all spectra were obtained in $CDCl_3$ and chemical shifts are reported in parts per million relative to TMS. Low-resolution mass spectral data was obtained for all compounds using a Bruker Daltonics Esquire electrospray–ion trap mass spectrometer. High-resolution mass spectral data was obtained on a Bruker Daltonics APEX III 47e Fourier transform (Ion Cyclotron Resonance) Mass Spectrometer for two key compounds of the library, compounds **5** and **21**. (Compound **5**: HR-ESI-MS m/z 369.1426 calculated for $C_{18}H_{22}N_2O_5Na$ $[M+Na]^+$, found 369.1427. Compound **21**: HR-ESI-MS m/z 417.1063 calculated for $C_{21}H_{18}N_2O_6Na$ $[M+Na]^+$, found 417.1068.)

({3-[Amino(oxo)acetyl]-1-(biphenyl-2-ylmethyl)-2-methyl-1*H*-indol-4-yl}oxy) acetic acid (Me-Indoxam). Prepared according to the literature procedure[33] except that the starting material used was the commercially available 4-hydroxy-2-methylindole **(A)** from TCI America. ^1H NMR (300 MHz, DMSO-d_6, δ): 2.35 (s, 3H), 4.66 (s, 2H), 6.36 (s, 2H), 6.40 (d, 1H), 6.51 (d, 1H), 6.88 (d, 1H), 7.02 (t, 1H), 7.19–7.58 (m, 8H), 7.73 (s, 1H), 12.90 (br s, 1H).

***tert*-Butyl [(2-methyl-1*H*-indol-4-yl)oxy]acetate (B)**. The commercially available 4-hydroxy-2-methylindole **(A)** (3.00 g, 20.38 mmol) and *t*-butylbromoacetate (3.98 g, 20.38 mmol) were dissolved in 100 mL acetone (freshly distilled from $CaSO_4$) in a 250 mL round bottom flask. To this solution at room temperature was added anhydrous potassium carbonate (5.66 g, 40.80 mmol) and the stirred mixture brought to reflux for 12 h. The solid was removed by filtration and washed with two 20 mL portions of acetone. The solvent was removed by rotary evaporation to leave an off-white solid. This solid was dissolved in 50 mL EtOAc and washed with 50 mL of a brine solution in a separatory funnel. The aqueous phase was extracted twice with 20 mL portions of EtOAc and the organic layers combined, dried over $MgSO_4$ and evaporated to leave an off-white solid. The product was purified by flash column chromatography on silica gel using 20% EtOAc/hexanes as eluant to give 4.131 g of a white powder (77% yield). This compound decomposes quickly in solution when not under argon. The product of decomposition is a bright green color. Therefore, it is imperative to work quickly, including the purification step. ^{1}H NMR (200 MHz, $CDCl_3$, δ): 1.51 (s, 9H), 2.42 (s, 3H), 4.65 (s, 2H), 6.40–6.47 (m, 2H), 6.85 (d, 1H), 7.07 (t, 1H), 7.91 (br s, 1H).

^{14}C-Labeled *tert*-butyl ({3-[amino(oxo)acetyl]-2-methyl-1*H*-indol-4-yl}oxy)acetate (C). To ^{14}C-labeled oxalic acid solid (50 μCi, 10 mCi/mmol) from American Radiolabeled Chemicals Inc. in an amber vial under argon atmosphere was added freshly distilled, unlabeled oxalyl chloride (185 μL, 2.12 mmol) and approximately 3 mg of phosphorus pentachloride solid. The exact weight of the phosphorus pentachloride could not be obtained, as it is sensitive to moisture, which causes the weight to change rapidly. The mixture was refluxed for 10 min until the evolution of bubbles had ceased upon standing at room temperature. The entire contents of the vial were transferred to a 1 L round bottom flask containing 400 mL freshly distilled CH_2Cl_2. Compound **(B)** (0.490 g, 1.86 mmol) was added as a solution in 100 mL freshly distilled CH_2Cl_2 over 1 h under an argon atmosphere via addition funnel. The bright yellow solution was left to stir for 8 h at room temperature before ammonia gas was bubbled into the solution for 15 min, at which point the mixture became pale yellow and a fluffy white solid precipitated. The precipitate was removed by filtration and the solvent removed by rotary evaporation to leave a yellow solid. The crude solid was dissolved in 150 mL EtOAc and washed with water followed by brine. The organic layer was dried over $MgSO_4$ and purified by column chromatography on silica gel using EtOAc as the eluant. The product was obtained in 87% yield as a bright yellow powder with a specific activity of 7160 cpm/μmol. ^{1}H NMR (200 MHz, CD_3OD, δ): 1.46 (s, 9H), 2.58 (s, 3H), 4.61 (s, 2H), 6.50 (dd, 1H), 6.98–7.12 (m, 2H).

Library synthesis of indole analogues (D). A collection of various alkyl bromides from Aldrich Chemicals was purchased in small quantities (10–12 mg each) and each was delivered in a separate 4 mL amber vial. These compounds were dissolved in 1.00 mL of freshly distilled THF and capped. When not in use the vials were stored at −20 °C in jars containing $CaSO_4$ as desiccant. Fifty μL of each of these solutions was added to individual 4 mL vials awaiting a reaction with compound **(C)**. A 4 mL vial was charged with compound **(C)** (20.0 mg, 0.06 mmol) and flushed with argon. The solid was dissolved in 2.25 mL freshly distilled THF. To this solution was added NaH (3.5 mg, 0.15 mmol) without mineral oil and the reaction left to stir at room temperature for 10 min, at which point it became a bright yellow color. The entire contents of the vial were removed by gas-tight syringe and 25 μL aliquots were added to each of the vials containing the alkyl bromide/THF solutions. These vials were then heated at 60 °C for 2 h followed by removal of solvent by entrainment with air. The vials containing the crude products were stored free of solvent at −20 °C until purified by HPLC. To each vial was added neat trifluoroacetic acid (100 μL, 1.30 mmol), vials were mixed on a vortex mixer for 15 s and left for 10 min at room temperature. The excess trifluoroacetic acid was removed by entrainment with air. The compounds were then purified using high performance liquid chromatography and eluting with a methanol/water/0.06% TFA system on a Vydac C-18 reverse phase semi-preparative 218TP1010 column using UV–Vis detection at 262 nm. The purified compounds were identified by electrospray mass spectrometry with characteristic fragmentation patterns. A speed vac (Savant Instruments) was used to remove the HPLC solvents from the fractions containing the desired products to leave solids. These solids were dissolved in 50 μL DMSO and transferred to Eppendorf tubes. An aliquot of this DMSO solution was used to quantify the compound using a liquid scintillation counter. Dilutions were made of each of the stock DMSO/inhibitor solutions in preparation for inhibition assays and stored at −20 °C.

***tert*-Butyl 4-[(2-methyl-1*H*-indol-5-yl)oxy]butanoate (F)**. A portion of 5-hydroxy-2-methylindole **(E)** (200.0 mg, 1.36 mmol) from Biosynth AG and *tert*-butyl 4-bromobutanoate (455 mg, 2.04 mmol) (prepared according to the literature procedure[61]) were dissolved in 20 mL acetone (freshly distilled from $CaSO_4$) in a 50 mL round bottom flask under argon. To this solution at room temperature was added anhydrous potassium carbonate (1.00 g, 6.8 mmol) and the stirred mixture brought to reflux for 3 days. The solid was removed by filtration and washed twice with 10 mL portions of acetone. The solvent was removed by rotary evaporation to leave a yellow oil. This oil was dissolved in 50 mL EtOAc and washed with 50 mL of brine in a separatory funnel. The aqueous phase was extracted with three 20 mL portions of EtOAc and the organic layers combined, dried over $MgSO_4$ and evaporated to leave a yellow oil. The product was purified by flash column chromatography on silica gel using 20% EtOAc/hexanes as eluant to give 359 mg (77% yield) of yellow oil. ^{1}H NMR (300 MHz, $CDCl_3$, δ): 1.49 (s, 9H), 2.04 (m, 2H), 2.42 (s, 3H), 2.46 (s, 2H), 4.03 (t, 2H), 6.12 (br s, 1H), 6.75 (dd, 1H), 6.99 (d, 1H), 7.17 (dd, 1H), 7.80 (br s, 1H).

^{14}C-Labeled *tert*-butyl 4-({3-[amino(oxo)acetyl]-2-methyl-1*H*-indol-5-yl}oxy)butanoate (G). To ^{14}C-labeled oxalic acid solid (50 μCi, 3 mCi/mmol) from American Radio-

labeled Chemicals Inc. in 1 mL dry CH_2Cl_2 in an amber vial was added freshly distilled, unlabeled oxalyl chloride (100 μL, 1.15 mmol) and approximately 3 mg of phosphorus pentachloride solid (see compound (**C**)). The mixture was refluxed for 30 min under an argon atmosphere and then the entire contents of the vial were transferred to a 1-liter round bottom flask containing 400 mL freshly distilled CH_2Cl_2. Compound **(F)** (219 mg, 0.756 mmol) was dissolved in 100 mL dry CH_2Cl_2 and added over 1 h under an argon atmosphere. The solution was left to stir for 12 h at room temperature before ammonia gas was bubbled into the solution for 15 min, at which point a white solid precipitated. The solid was removed by filtration and the solvent removed by rotary evaporation to leave an off white solid. The crude solid was dissolved in 100 mL EtOAc and washed with water followed by brine. The organic layer was dried over $MgSO_4$ and purified by column chromatography on silica gel using 75% EtOAc/hexanes as eluant. The product was obtained as an off-white powder with a specific activity of 11,723 cpm/μmol (85% yield). ^{1}H NMR (300 MHz, CD_3OD, δ): 1.43 (s, 9H), 2.03 (m, 2H), 2.42 (t, 2H), 2.64 (s, 3H), 4.00 (t, 2H), 6.81 (dd, 1H), 7.22 (dd, 1H), 7.61 (d, 1H).

Library synthesis of indole analogues (H). The alkyl bromides used in the generation of the first library were also used to generate this library of compounds. The alkyl bromides were stored as solutions in dry THF in a dessicated jar at −20 °C. Twenty-five μL aliquots of each of these solutions were added to individual 4 mL vials awaiting a reaction with compound **(G)**. A 4 mL vial was charged with compound **(G)** (20.0 mg, 0.06 mmol) and flushed with argon. The solid was dissolved in 4 mL freshly distilled THF. To this solution was added NaH (3.5 mg, 0.15 mmol) without mineral oil and the reaction left to stir at room temperature for 10 min, at which point the solution turned yellow-green. The entire contents of the vial were removed by syringe and 50 μL aliquots were added to each of the vials containing alkyl bromide/THF solutions. These vials were then placed in an oven at 60 °C for 2 h. The resultant compounds were treated in the same manner as for the generation of the first library, purified by HPLC, and characterized by electrospray ionization mass spectrometry. The compounds were quantified using liquid scintillation counting and DMSO/inhibitor stock solutions were made as for the first set of library compounds.

Microtiter plate assay of sPLA$_2$s for inhibition analysis. To each well of a 96-well microtiter plate was added 100 μL of solution A in assay buffer (27 μM bovine serum albumin, 50 mM KCl, 1 mM $CaCl_2$, 50 mM Tris–HCl, pH 8.0) followed by the desired concentration of $sPLA_2$ inhibitor ($\leq$3 μL in DMSO from serial diluted stock solutions) or 3 μL of DMSO only for control reactions. Solution B was prepared immediately prior to each set of assays, which consisted of only eight wells, to avoid loss of enzymatic activity due to sticking to the walls of the container. Solution B was delivered in 100 μL portions to all eight wells except the first well and had the same composition as Solution A plus 5–2000 ng of $sPLA_2$ (depending on specific enzymatic activity[42]). In place of Solution B was added an additional 100 μL portion of Solution A as a minus enzyme control to the first of the eight wells in the assay. Quickly after the addition of Solution B, the assay was initiated by the addition of 100 μL of Solution C (4.2 μM 1-hexadecanoyl-2-(1-pyrenedecanoyl)-*sn*-glycero-3-phosphoglycerol (Molecular Probes) vesicles in assay buffer) with a repeating pipettor to all eight wells. The fluorescence (excitation = 342 nm, emission = 395 nm) was read with a microtiter plate spectrophotometer (Fluorocount, Packard Instruments). Control reactions without enzyme or inhibitor were run with each assay of eight wells and the percent inhibition calculated from the initial slopes of fluorescence versus time. The amount of enzyme used per well are as follows: hGIB, 0.5 ng; hGIIA, 0.5 ng; hGIID, 200 ng; hGIIE, 500 ng; hGIIF, 30 ng; hGIII, 5 ng; hGIII, 5 ng; hgV, 1 ng; hGX, 1 ng; hGXIIA, 1,500 ng; mGIB, 1.6 ng; mGIIA, 8 ng; mGIIC, 12 ng; mGIID, 2,000 ng; mGIIE, 5 ng; mGIIF, 100 ng; mGV, 6 ng; mGX, 3.5 ng. All of the recombinant mouse and human $sPLA_2$s were prepared as described.[42]

References and notes

1. Waite, M. *The Phospholipases*; Plenum: New York, 1987.
2. Murakami, M.; Kudo, I. *J. Biochem.* **2002**, *131*, 285.
3. Dennis, E. A. *Am. J. Respir. Crit. Care Med.* **2000**, *161*, S32.
4. Valentin, E.; Lambeau, G. *Biochim. Biophys. Acta* **2000**, *1488*, 59.
5. Six, D. A.; Dennis, E. A. *Biochim. Biophys. Acta* **2000**, *1488*, 1.
6. Jain, M. K.; Yuan, W.; Gelb, M. H. *Biochemistry* **1989**, *28*, 4135.
7. Gelb, M. H.; Jain, M. K.; Hanel, A. M.; Berg, O. *Ann. Rev. Biochem.* **1995**, *64*, 653.
8. Gelb, M. H.; Jain, M. K.; Berg, O. *Faseb J.* **1994**, *8*, 916.
9. Berg, O. G.; Jain, M. K. *Interfacial Enzyme Kinetics*; Wiley: West Sussex, England, 2002.
10. Beaton, H. G.; Bennion, C.; Connolly, S.; Cook, A. R.; Gensmantel, N. P.; Hallam, C.; Hardy, K.; Hitchin, B.; Jackson, C. G.; Robinson, D. H. *J. Med. Chem.* **1994**, *37*, 557.
11. Lin, H.-K.; Gelb, M. H. *J. Am. Chem. Soc.* **1993**, *115*, 3932.
12. De Haas, G. H.; Dijkman, R.; Lugtigheid, R. B.; Dekker, N.; Van Den Berg, L.; Egmond, M. R.; Verheij, H. M. *Biochim. Biophys. Acta* **1993**, *1167*, 281.
13. Jain, M. K.; Tao, W.; Rogers, J.; Arenson, C.; Eibl, H. et al. *Biochemistry* **1991**, *30*, 10256.
14. Davidson, F. F.; Hajdu, J.; Dennis, E. A. *Biochem. Biophys. Res. Commun.* **1986**, *137*, 587.
15. Chandra, V.; Jasti, J.; Kaur, P.; Srinivasan, A.; Betzel, C.; Singh, T. P. *Biochemistry* **2002**, *41*, 10914.
16. Breitenstein, W.; Marki, F.; Roggo, S.; Wiesenberg, I.; Pfeilschifter, J. et al. *Eur. J. Med. Chem.* **1994**, *29*.
17. Bryant, M. D.; Flick, K. E. S. K.R.; Wilton, D. C.; Stoddard, B. L.; Gelb, M. H. *Bioorg. Med. Chem. Lett.* **1999**, *9*, 1097.
18. Jain, M. K.; Ghomashchi, F.; Yu, B.-Z.; Bayburt, T.; Murphy, D. et al. *J. Med. Chem.* **1992**, 3584.
19. Marshall, L. A.; Hall, R. H.; Winkler, J. D.; Badger, A.; Bolognese, B. et al. *J. Pharmacol. Exp. Ther.* **1995**, *274*, 1254.

20. Jain, M. K.; Yu, B.-Z.; Rogers, J. M.; Smith, A. E.; Boger, E. T. et al. *Phytochemistry* **1995**, *39*, 537.
21. LeMahieu, R. A.; Carson, M.; Han, R.-J.; Madison, V. S.; Hope, W. C. et al. *J. Med. Chem.* **1993**, *36*, 3029.
22. Burke, J. R.; Gregor, K. R.; Tramposch, K. M. *J. Biol. Chem.* **1995**, *270*, 274.
23. Yoshida, T.; Nakamoto, S.; Sakazaki, R.; Matsumoto, K.; Terui, Y. et al. *J. Antibiot. Tokyo* **1991**, *44*, 1467.
24. Tanaka, K.; Matsutani, S.; Kanda, A.; Kato, T.; Yoshida, T. *J. Antibiot.* **1994**, *47*, 631.
25. Genisson, Y.; Tyler, P. C.; Young, R. N. *J. Am. Chem. Soc.* **1994**, *116*, 759.
26. Hite, G. A.; Mihelich, E. D.; Tulio, S.; Edmund, W. S. *European Patent*; 0 846 687 A1, 1998.
27. Chandra, V.; Jasti, J.; Kaur, P.; Dey, S.; Srinivasan, A. et al. *Acta Crystallogr. D Biol. Crystallogr.* **2002**, *58*, 1813.
28. Chandra, V.; Jasti, J.; Kaur, P.; Dey, S.; Perbandt, M. et al. *J. Biol. Chem.* **2002**, *277*, 41079.
29. Chandra, V.; Jasti, J.; Kaur, P.; Betzel, C.; Srinivasan, A. et al. *J. Mol. Biol.* **2002**, *320*, 215.
30. Schevitz, R. W.; Bach, N. J.; Carlson, D. G.; Chirgadze, N. Y.; Clawson, D. K. et al. *Nat. Struct. Biol.* **1995**, *2*, 458.
31. Mihelich, E. D.; Schevitz, R. W. *Biochim. Biophys. Acta* **1999**, *1441*, 223.
32. Dillard, R. D.; Bach, N. J.; Draheim, S. E.; Berry, D. R.; Carlson, D. G. et al. *J. Med. Chem.* **1996**, *39*, 5119.
33. Draheim, S. E.; Bach, N. J.; Dillard, R. D.; Berry, D. R.; Carlson, D. G. et al. *J. Med. Chem.* **1996**, *39*, 5159.
34. Scott, D. L.; White, S. P.; Otwinowski, Z.; Yuan, W.; Gelb, M. H. et al. *Science* **1990**, *250*, 1541.
35. White, S. P.; Scott, D. L.; Otwinowski, Z.; Gelb, M. H.; Sigler, P. B. *Science* **1990**, *250*, 1560.
36. Scott, D. L.; Otwinowski, Z.; Gelb, M. H.; Sigler, P. B. *Science* **1990**, *250*, 1563.
37. Scott, D. L.; White, S. P.; Browning, J. L.; Rosa, J. J.; Gelb, M. H. et al. *Science* **1991**, *254*, 1007.
38. Thunnissen, M. M. G. M.; Ab, E.; Kalk, K. H.; Drenth, J.; Dijkstra, B. W. et al. *Nature* **1990**, *347*, 689.
39. Cha, S. S.; Lee, D.; Adams, J.; Kurdyla, J. T.; Jones, C. S. et al. *J. Med. Chem.* **1996**, *39*, 3878.
40. Kitadokoro, K.; Hagishita, S.; Sato, T.; Ohtani, M.; Miki, K. *J. Biochem.* **1998**, *123*, 619.
41. Ying, H. P.; Epstein, T. M.; Jain, M. K.; Bahnson, B. J. *Biochemistry* **2001**, *40*, 609.
42. Singer, A. G.; Ghomashchi, F.; Le Calvez, C.; Bollinger, J. G.; Bezzine, S. et al. *J. Biol. Chem.* **2002**, *277*, 48535.
43. Bezzine, S.; Koduri, R. S.; Valentin, E.; Murakami, M.; Kudo, I. et al. *J. Biol. Chem.* **2000**, *275*, 3179.
44. Bezzine, S.; Bollinger, J. G.; Veatch, S. L.; Keller, S. L.; Gelb, M. H. *J. Biol. Chem.* **2002**, *277*, 48523.
45. Han, S. K.; Kim, K. P.; Koduri, R. S.; Bittova, L.; Munoz, N. M. et al. *J. Biol. Chem.* **1999**, *274*, 11881.
46. Kim, K. P.; Rafter, J. D.; Bittova, L.; Han, S. K.; Snitko, Y. et al. *J. Biol. Chem.* **2001**, *276*, 11126.
47. Hanasaki, K.; Ono, T.; Saiga, A.; Morioka, Y.; Ikeda, M. et al. *J. Biol. Chem.* **1999**, *274*, 34203.
48. Morioka, Y.; Saiga, A.; Yokota, Y.; Suzuki, N.; Ikeda, M. et al. *Arch. Biochem. Biophys.* **2000**, *381*, 31.
49. Balboa, M. A.; Balsinde, J.; Winstead, M. V.; Tischfield, J. A.; Dennis, E. A. *J. Biol. Chem.* **1996**, *271*, 32381.
50. Hanasaki, K.; Yamada, K.; Yamamoto, S.; Ishimoto, Y.; Saiga, A.; Ono, T.; Ikeda, M.; Notoya, M.; Kamitani, S.; Arita, H. *J. Biol. Chem.* **2002**, *277*, 29116.
51. Gesquiere, L.; Cho, W.; Subbaiah, P. V. *Biochemistry* **2002**, *41*, 4911.
52. Pan, Y. H.; Yu, B.-Z.; Singer, A. G.; Ghomashchi, F.; Lambeau, G. et al. *J. Biol. Chem.* **2002**, *277*, 29086.
53. Scott, D. L.; Sigler, P. B. *Adv. Protein Chem.* **1994**, *45*, 53.
54. Dillard, R. D.; Bach, N. J.; Draheim, S. E.; Berry, D. R.; Carlson, D. G.; Chirgadze, N. Y.; Clawson, D. K. et al. *J. Med. Chem.* **1996**, *39*, 5137.
55. Burley, S. K.; Petsko, G. A. *Science* **1985**, *229*, 23.
56. Otwinowski, Z.; Minor, W. *Methods Enzymol.* **1997**, *276*, 307.
57. Navazza, J. *Acta Cryst.* **1994**, *A50*, 157.
58. Brunger, A. T.; Adams, P. D.; Clore, G. M.; Delano, W. L.; Gros, P. et al. *Acta Cryst.* **1998**, *D54*, 905.
59. Sack, J. S.; Quiocho, F. A. *Methods Enzymol.* **1997**, *277*, 158.
60. Jones, T. A.; Zou, J.-Y.; Cowan, S. W. *Acta Cryst.* **1991**, *A47*, 110.
61. Morin, C.; Vidal, M. *Tetrahedron* **1992**, *48*, 9277.
62. Kraulis, P. *J. Appl. Cryst.* **1991**, *24*, 946.